Molecular dynamics simulation for investigating and assessing reaction conditions between carboxylated polyethersulfone and polyethyleneimine

Rahmati, Mahmoud ; Rajabzadeh, Saeid ; Abdelrasoul, Amira ; Kawabata, Yuki ; Yoshioka, Tomohisa ; Matsuyama, Hideto ; Mohammadi, Toraj

(Citation)
Journal of Applied Polymer Science,138(44):51304

(Issue Date)
2021-06-25

(Resource Type)
journal article

(Version)
Accepted Manuscript

Molecular Dynamics Simulation for Investigating and Assessing Reaction Conditions between Carboxylated Polyethersulfone and Polyethyleneimine

Mahmoud Rahmati[a]*, Saeid Rajabzadeh[b], Amira Abdelrasoul[c], Yuki Kawabata[b], Tomohisa Yoshioka[b], Hideto Matsuyama[b], Toraj Mohammadi[d]**

[a] Department of Chemical Engineering, Graduate University of Advanced Technology, Kerman, Iran

[b] Research Center for Membrane and Film Technology, Department of Chemical Science and Engineering, Kobe University, Rokkodaicho 1-1, Nada, Kobe, 657-8501, Japan

[c] Department of Chemical and Biological Engineering, University of Saskatchewan, 57 Campus Drive, Saskatoon, Saskatchewan, S7N 5A9, Canada

[d] Center of Excellence for Membrane Science and Technology, Department of Chemical, Petroleum and Gas Engineering, Iran University of Science and Technology (IUST), Narmak, Tehran, Iran

* First corresponding author: Mahmoud Rahmati, Department of Chemical Engineering, Graduate University of Advanced Technology, Kerman, Iran; E-mail address: m.rahmati@kgut.ac.ir

** Second corresponding author: Saeid Rajabzadeh, Research Center for Membrane and Film Technology, Department of Chemical Science and Engineering, Kobe University, Rokkodaicho 1-1, Nada, Kobe, 657-8501, Japan; E-mail address: rajabzadehk@people.kobe-u.ac.jp

Abstract

Recently, Nano-filtration membranes are made by the reaction between a reactive functional group on the surface of a tight ultrafiltration membrane and a charged branched polymer. This reaction makes the selective layer of the nanofiltration membrane, which plays an essential role in membrane performance. A molecular dynamics simulation with a reactive force field was used to investigate the reaction of carboxylated polyethersulfone as the functional group of the ultrafiltration membrane with polyethyleneimine. Experimental elucidation of the reaction between the PEI amine and carboxyl groups is challenging, and an MD simulation was thus employed. Furthermore, the simulation results show that the PEI and carboxylated polyethersulfone polymers react with each other in a temperature-dependent manner. While no reaction occurs at 298 K, carboxylated polyethersulfone and PEI begin to react when the temperature is increased from 298 K to 323 K. Furthermore, a reversible reaction was observed with a subsequent increase in temperature to 353 K.

1. Introduction

Nano-filtration (NF) membranes have been synthesised using a variety of methods. A typical and well-developed method that has been widely applied for NF membrane fabrication is interfacial polymerisation (IP) [1-3]. Organic acid and base monomers react at the mouth of the ultrafiltration (UF) or microfiltration (MF) membrane pore to create an NF membrane in the IP method. Although different types of monomers, including both acidic and basic monomers, have been applied with the addition of some type of additives, the primary mechanism that comprises

the organic acid-base reaction in the mouth of the pores is complex and results in a sharp reduction in the pore size. On tightening the base membrane (UF or MF membranes) pores, the pore size drastically decreases to the NF-membrane pore-size range of 1 to 10 nm. Recently, a new method for the fabrication of NF membranes has been under development mainly for brackish water softening [4-8]. In this method, a reactive functional group on the surface of a tight UF membrane reacts with a charged branched polymer. This reaction not only causes the UF membrane pore size to become much smaller in the range of the NF membranes, but also results in the fabrication of a membrane that has a considerable charge and is suitable for water softening and removal of divalent and multivalent charges.

Setiawan et al. [9] fabricated positive-surface-charge NF membranes using a dual-layer membrane with a skinny layer of a special poly(amide-imide), Torlon^{R}, as the selection layer on the porous support layer of the polyethersulfone (PES). Polyallylamine was used as a polycation to react with Torlon on the support UF membrane surface to the make selective skin layer, to obtain a positively charged NF membrane. In another research, Han et al. [10] developed positively charged NF membranes using Torlon/sulfonated polyphenylene sulfone as based blend UF membrane and implemented a subsequent reaction of the UF base membrane with hyperbranched PEI to obtain the NF membrane.

Recently, we fabricated a positively charged NF membrane based on the reaction of the branched or hyperbranched polycation (polyethyleneimine (PEI)) with the carboxylic group on the surface of the blend PES/C-PES UF membrane [7,8]. Furthermore, by blending the PES and synthesised carboxylaed PES (C-PES), a UF membrane with carboxyl functional groups on the membrane surface was fabricated such that it could react with branched or hyperbranched poly-cations (PEI) to fabricate a positively charged NF membrane. The influence of the blending ratio

of the PES and C-PES, reaction temperature, reaction time, PEI solution pH, supporting polyelectrolyte concentration (NaCl concentration in PEI solution), and PEI cross-linking concentration and time were studied for the evaluation of our novel prepared membrane. Although several characterisation techniques were used to thoroughly understand the formation mechanism of the active layer, an accurate and precise understanding could not be realised. For example, the membrane surface was analysed using Fourier transform infrared spectroscopy–attenuated total reflectance (FTIR-ATR) to determine the formed covalent bond between the PEI; nevertheless, identifying the carboxyl group was difficult for several reasons. Firstly, the number of segregated COOH groups at the membrane surface was significantly low. Secondly, among the large number of amine groups of PEI, very few of them from a big molecule with the COOH group. Lastly, the penetration depth of the infrared wave inside the membrane in the FTIR-ATR analysis was approximately a few microns, which is much deeper than the dense skin layer formed on the membrane (several nanometers) based on the molecular reaction. Therefore, the FTIR-ATR spectra comprise an average of the detected bonds at the depth of a few microns of the membrane. However, the thickness of the formed dense selective layer owing to the reaction of the molecules remains less than several nanometers. Thus, realising the recognition of the thin dense selective layer formed based on the carboxyl group that reacted with the amine group of PEI in the membrane's dense selective layer by using FTIR-ATR is difficult. This resulted in an unapproved analysis of the covalent bond between COOH and the amine group.

Furthermore, in our recent studies[7,8], we observed that X-ray photoelectron spectroscopy was an impractical approach for confirming the reaction owing to very low intensity of the reaction peak. Therefore, the formation of the covalent bond between an amine and COOH group was

hypothesised based on other experimental analysis as well as some explanations and justifications. A similar phenomenon was observed in a study by Fang et al. [11].

In this study, we tried to use an MD simulation to obtain a clear and deep understanding of the interaction between the amine group from the PEI and the COOH group from the C-PES that results in the formation of the selective skin layer of the NF membrane. In the recent decades of MD simulation development, reactive force fields such as the Tersoff potential, reactive empirical bond order, and reactive force field (ReaxFF) have been created using the bond-order concept. These bond-order force fields equip software by considering the formation and dissociation of chemical bonds during the MD simulations. Therefore, chemical reactions can be modeled. ReaxFF has been applied for a wide range of chemical reactions, especially thermal decomposition[12], cross-linking[13-16], polymerisation of polymer matrix[17], mechanical properties[16], membrane[18] and thermo-mechanical properties [19] of polymers [20]. For example, Hu et al. 21 investigated the thermal-decomposition initiation mechanisms and kinetics of poly(methyl styrene) using MD simulations with the ReaxFF reactive force field. It was reported that the thermal decomposition of the poly(methyl styrene) molecule is initiated mainly by a carbon-carbon sharp distance gap and is accompanied by degradation reactions that result in the formation of degradation products.

The mechanical properties of the amorphous and crystalline phases of polyether–ether–ketone (PEEK) were studied by Pisan et al. [22] using an MD simulation and reactive force fields. The study demonstrated that the bulk mechanical properties of PEEK have good agreement with the experimental data. Odegard et al. [16] used an MD simulation with ReaxFF to study the mechanical behavior of crosslinked epoxy resins. Their results clearly demonstrated that the mechanical stiffness and strength values of epoxy resins show close agreement with the

experimental values. Chenoweth et al. [23] examined the temperature and pressure dependence of poly(dimethylsiloxane) polymer decomposition to investigate the chemical stability of polymers. The simulation results of Zhao et al. [24] demonstrated that the MD simulation with ReaxFF is a reliable method for the evaluation of the chemical reaction mechanisms in polycarbonate pyrolysis, activation energy, and pre-exponential factor, which agreed with the experimental findings.

Therefore, the objective of the present study is to use the ReaxFF for the first time to investigate the chemical reaction between the PEI and C-PES polymers in the presence of water at the atomic level to fabricate an NF-membrane selective dense layer. For this purpose, first, the density and radial distribution function (RDF) analysis of PEI, C-PES and water in the pure state were investigated using reactive MD simulation, and the simulation results were compared with experimental data. The chemical reaction between the PEI and C-PES polymers were then simulated to confirm our hypothesis, which we had used to explain the phenomena reported in our previously published paper [8].

2. Computational Methods

The reactive MD simulations was conducted to investigate the chemical reaction between the PEI and C-PES polymers in the presence of water at various temperatures. The computational method approach consists of the two the reactive MD simulation, and properties.

2.1. Reactive MD Simulation

ReaxFF is used in the simulation of the chemical reaction in the MD simulation. This force filed is a general bond-order-dependent that provides accurate descriptions of the bond formation and breakage. Despite conventional unreactive force fields, in ReaxFF, the connectivity of the

atoms is determined, and a calculation is performed based on the atoms' bond. The interatomic distances are updated in each MD step, which allows bonds to break or form during the simulation. Non-bonded interactions, such as van der Waals and Coulomb interactions are calculated between each pair of atoms regardless of their connection.

The total energy of the system in the case of ReaxFF is expressed in Equation (1) [19-21].

$$E_t = E_{bond} + E_{over} + E_{under} + E_{val} + E_{angle} + E_{tors} + E_{vdw} + E_{coulmb} + E_{lp} + E_{H-bond} + E_{rest}$$

Equation (1)

where the total energy of the system (E_t) consists of the bond energy (E_{bond}), over coordination energy (E_{over}), undercoordination energy (E_{under}), valence-angle energy (E_{val}), angle strain energy (E_{angle}), torsion angle energy (E_{tors}), van der Waals energy (E_{vdW}), Coulomb energy ($E_{Coulomb}$), lone pair energy (E_{lp}), hydrogen bond interactions energy ($E_{H\text{-}bond}$), and restrain energy (E_{rest}). The ReaxFF coefficients of the C, H, N, O, and S atoms were adopted in all the simulations from a previously reported study [25].

The Nose-Hoover[21,26-28] thermostat and Berendsen barostat [16] were employed to control the pressure and temperature during the simulations with a decay constant of 0.1 ps [29]. The Ewald summation method, with an accuracy of 0.001 kcal/mol, was used for the long-range Coulomb interactions [25]. The cutoff distance of the Van der Waals interaction was considered to be 1.25 nm [27]. The Large-scale Atomic/Molecular Massively Parallel Simulator (LAMMPS) open source package. The velocity Verlet algorithm and the time step of 0.1 fs [16,21] were used to all MD simulations. The periodic boundary condition is used in all the simulation boxes.

2.2. Properties

At first, the models of the molecular structure of the monomers and polymeric chains of PEI and C-PES were fabricated to build the simulation box and run the MD simulation, as schematically represented in Fig. 1. The polymer chains of PEI and C-PES were used in the all simulations include 20 monomers. Finally, the density pure materials(PEI, C-PES and water) and the reaction between the polymers were investigated.

2.2.1. Density

The density of pure PEI, C-PES, and water was calculated using MD simulation. For this purpose, the amorphous cell module in the Materials Studio software [30] was applied for preparing the simulation boxes and the initial density of them was 0.1 g/cm^3 [27]. The simulation boxes of pure PEI, C-PES, and water contain 10, 10, and 100 molecules, respectively. After constructing the simulation box, a 500 ps MD simulation with a time step of 0.1 fs and using ReaxFF was performed on the simulation box in the NPT ensemble to reach the final equilibrium density at 1 bar and 298 K. Finally, the numerical mean density is calculated from the simulation time of 250 ps onwards and it is reported as the equilibrium density of the polymer or water.

2.2.2. Chemical Reaction

For the reactive MD simulation of the chemical reaction of the PEI and C-PES polymers, a simulation box with a density of 0.4 g/cm^3 is constructed and contains 1, 1, and 30 molecules of PEI, C-PES, and water, respectively, and it is called a reaction system. The simulation procedure began with the minimisation of the reaction system using the conjugate gradient algorithm with a force tolerance of 1 kcal/mol/Å, after constructing the simulation box. The reaction system was then equilibrated using the NVT ensemble and MD simulation with ReaxFF at 298 K for a running

time of 10 ps. Finally, MD simulations were performed for 10 ns on the reaction system under the NVT ensemble and periodic conditions at 298 K to generate the stable system. The simulation results of the system were recorded every 1000 fs.

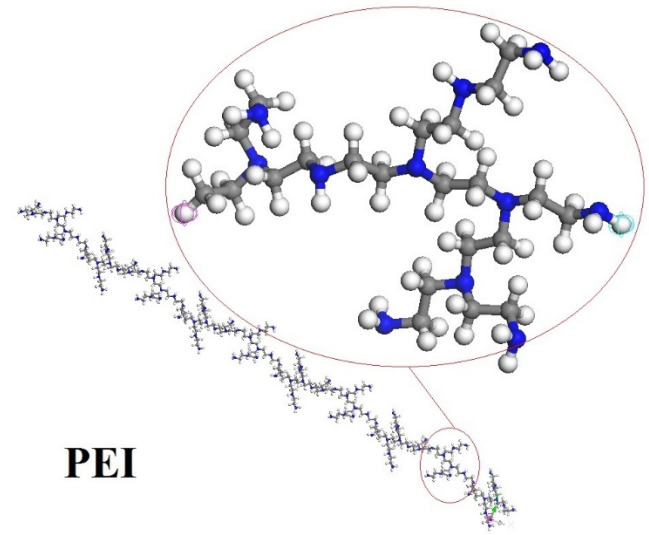

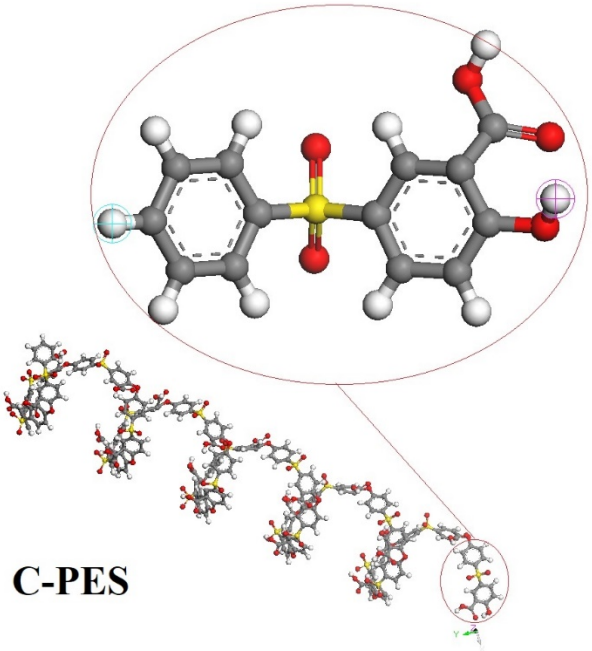

Fig. 1: Chemical structure of PEI and C-PES monomers (circles) and polymer chains (the colors blue, red, yellow, white, and gray represent nitrogen, oxygen, sulfur, hydrogen, and carbon, respectively).

3. Results and Discussion

3.1. Validation of MD Simulation Results

The pure density of the water, PEI and C-PES polymers were calculated using the MD simulation and ReaxFF force fields. In this study, owing to the very low carboxylation degree of polyethersulfone (PES), it was assumed that the density of C-PES is equal to the density of the PES polymer. The experimental density for the pure PEI, C-PES, and water at 298 K and 1 bar are 1.02 [31], 1.24 [32], and 0.998 g/cm^3, respectively. The simulation results show that the average density of the PEI polymer is 1.05 g/cm^3 for the ReaxFF, which are in good agreement with the experimental value of 1.02 g/cm^3. Furthermore, the average density of water is 0.96 g/cm^3 when using and ReaxFF, which was in agreement with the experimental value of 0.99 g/cm^3. In addition, the experimental density of C-PES is 1.24 g/cm^3, which is similar to the simulation results obtained using the ReaxFF. Nevertheless, as the degree of polymerisation in the MD simulation is much lower than the degree of polymerisation in the experiment, there is little difference between the simulation result and the experimental data. Therefore, the MD simulation results are in good agreement with the experimental data.

The RDF shows the probability of the presence of atoms A near atoms B at the distance *r* ($g_{A\text{-}B}(r)$), which was averaged over the MD trajectories using Equation (2) [33,34]

$$g_{A-B} = \frac{(\frac{n_B}{4\pi r^2 \Delta r})}{(\frac{N_B}{V})} \quad \text{Equation (2)}$$

where n_B is the number of atoms B around atoms A that are located inside a spherical shell of thickness Δr, N_B is the total number of atoms B, and V is the total system volume.

The RDFs of H–O and O–O of the water atoms are presented in Fig. 2. As presented in Fig. 2, the first sharp peak at 1 Å indicated the chemical bond between the O and H atoms and this value is in good agreement with the ab initio value of 0.958 Å [35] and the MD simulation value of 1 Å [35,36]. The other peaks at 1.7 [35] and 3.3 Å represented the hydrogen bonds between the water molecules. The RDFs of O–O water molecules in Fig. 2b indicate that there are two peaks at 2.8 [36] and 4.5 Å, which indicates the hydrogen bonds between the water molecules, and they are similar to the results reported in the previous study [35-37]. The value of first sharp peak of RDF of O–O water molecules (2.8 Å) is in good agreement with the ab initio BLYP, ReaxFF MD and experimental data value of 2.80 [38,39], 2.77 [36] and 2.82 [40] Å, respectively.

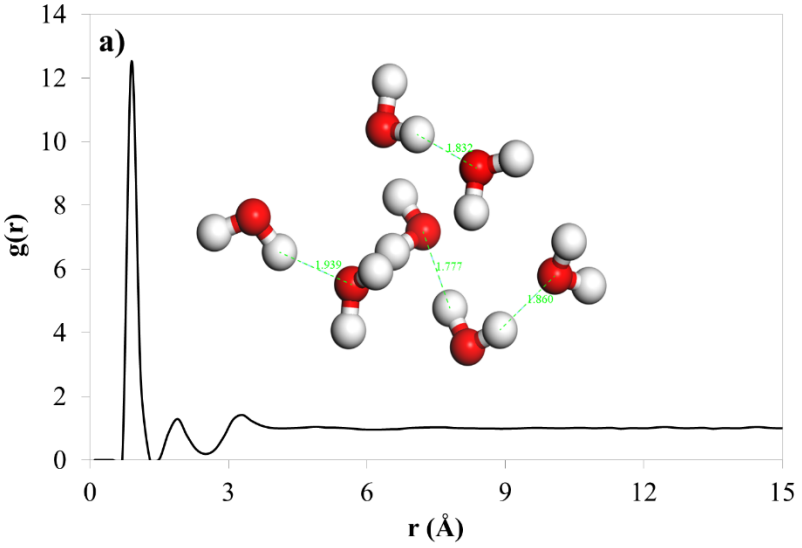

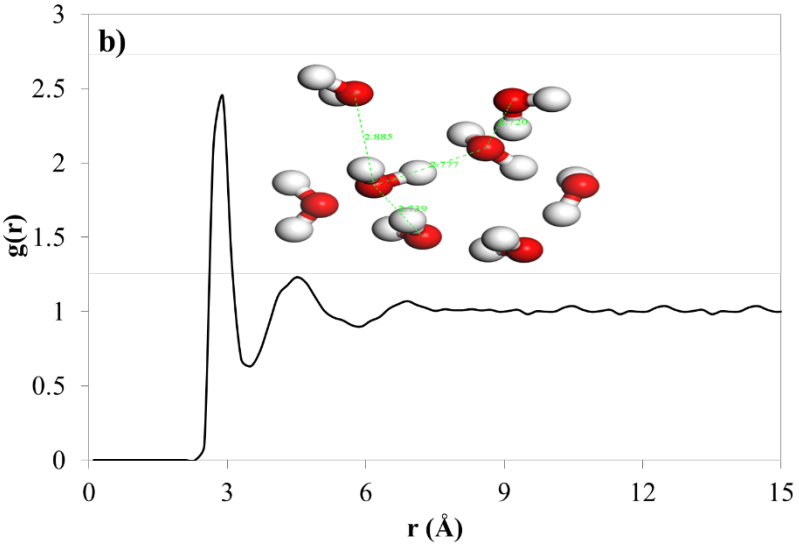

Fig. 2: RDFs of water molecules: a) H–O; and b) O–O.

The RDFs of the H–N, C–N, C–C, and C–H of PEI polymer atoms are presented in Fig. 3. The RDF results presented in Fig. 3a show the existence of three peaks; the first sharp peaks at 1.1 Å are those of the N–H bonds in the nitrogen atoms bonded by one or two carbon atoms. The second sharp peak occurs at 2.1 Å is indicative of the distance between the nitrogen and hydrogen atoms in the H–C–N bonds, and the third peak at 2.7 Å indicates the distance between the nitrogen and hydrogen atoms in the H–C–C–N bonds. The RDF of the C–N bond in Fig. 3b indicate that the two sharp peaks at 1.5 and 2.5 Å, respectively, are related to the distance between the nitrogen and carbon atoms that are bonded and non-bonded in the polymer chain. According to the experimental data [41], the bond length of N-C is 1.45 Å which is in good agreement with this RDF results. In addition, the results presented in Figs. 3c and d show two sharp peaks at 1.5 and 1.1 Å, which indicate the C–C and C–H bonds in the PEI polymer chain, respectively, and these value are in goog agrement with the ReaxFF MD simulation results an the experimental data [27].

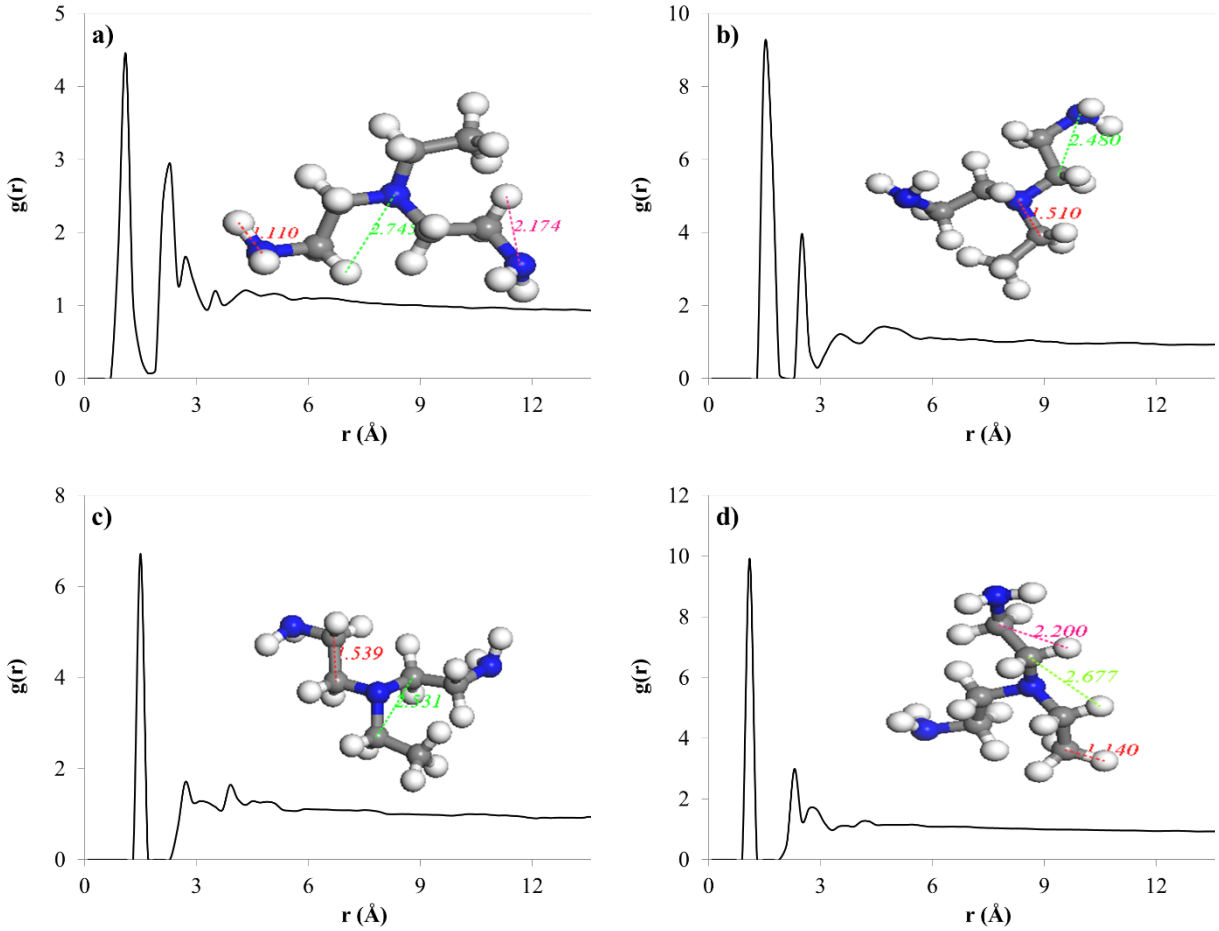

Fig. 3: RDFs of PEI polymer atoms: a) H–N; b) C–N; c) C–C; and d) C–H.

Fig. 4 presents the RDFs of the C-PES polymer atoms. As shown in Fig. 4a, the positions of the peaks in the H–O RDFs are located at 1 and 2.7 Å, wherein the first peak represents the chemical bond between the O and H atoms in the C-PES chains. The RDF of C-C in Fig. 4c, shows there are two sharp peaks at 1.6 and 2.6 Å corresponds to the sp^2–sp^2 bonds and the nearest neighbor in the carbon ring, respectively, and these values are in good agreement with the previous ReaxFF MD simulation [26]. Furthermore, the RDF results in Figs. 4 c, and d show that the first peaks are located at 1.5, and 1.5 Å, which indicate the chemical bonds of C–C, and S–O, respectively.

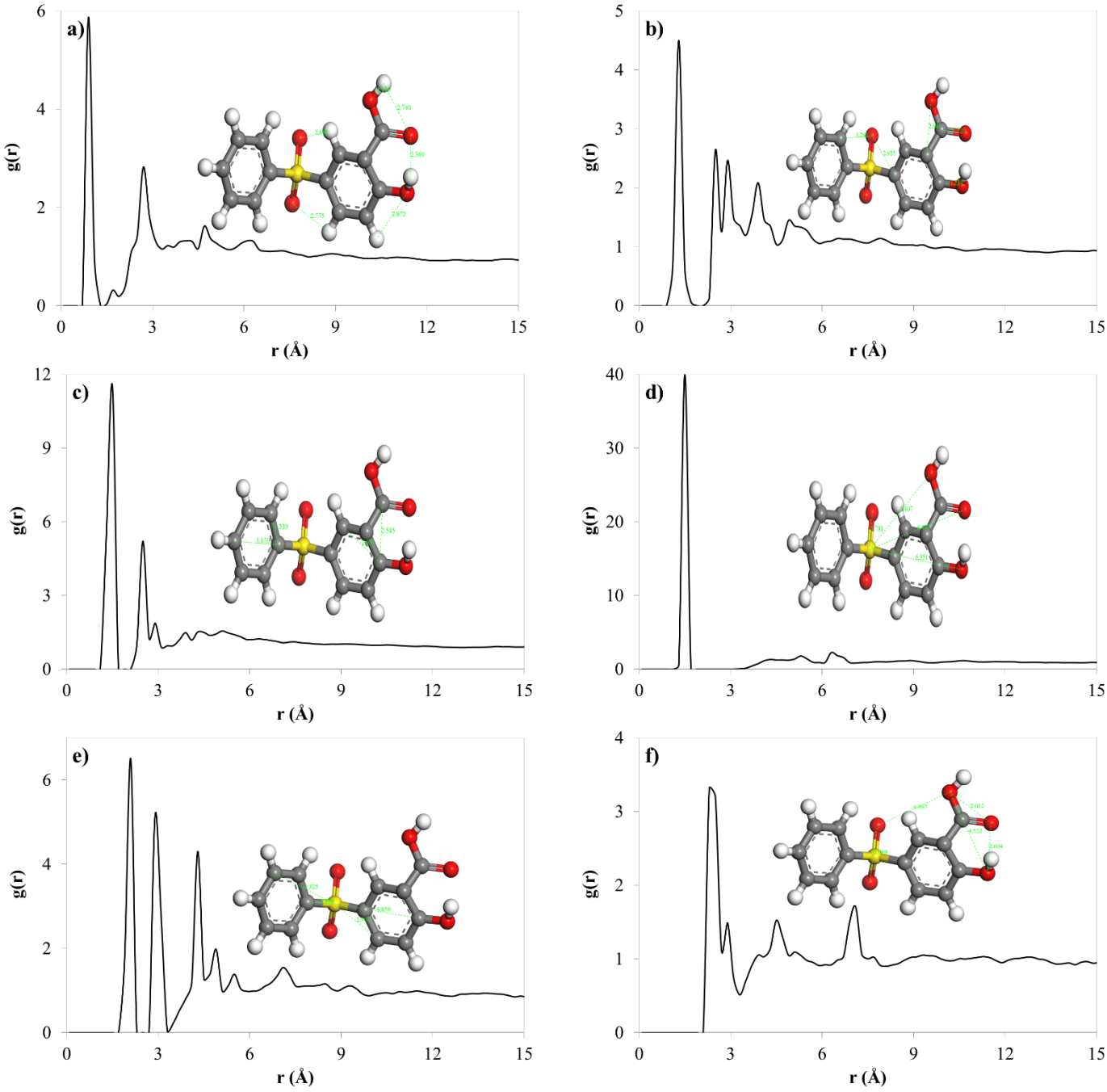

Fig. 4: RDFs of C-PES polymer atoms interactions. a) H–O; b) C–O; c) C–C; d) S–O; e) S–C; and f) O–O.

Finally, it can be concluded that, according to the density results of pure polymer and water, the simulation results are in good agreement with the experimental data and also the RDF results

in Figs. 2, 3 and 4, which confirms that the used ReaxFF parameters of the aforementioned previous study [25] are appropriate for the MD simulation of the chemical reaction between the PEI and C-PES polymers.

3.2. Chemical Reaction

The calculation of the total number of molecules during the reactive MD simulation is an effective method of examining the possibility of the molecular reactions. Therefore, the total number of molecules, including the PEI and C-PES polymers and the water molecules, water molecules, and the type of molecules in the MD simulation were calculated at the beginning of the simulation (1 ns from the total simulation time), and the results are presented in Fig. 5. The simulation results indicate that the total number of molecules in the simulation box decreases over time, and for 500 ps, the variation in the total number of molecules was reduced. The total number of molecules in the simulation box before running the reactive simulation was 32 molecules, which comprised 30 water molecules, one PEI molecule, and one C-PES molecule. The presence of nitrogen atoms in the PEI polymer causes the latter to have a very high affinity for water molecules, and thus, the water molecules decompose into H^+ and OH^-, and they are then bonded to the N atom of the polymer chain. Therefore, at the beginning of the simulation, the total number of molecules increases slightly and subsequently decreases.

According to the results in Fig. 5a, the total number of molecules at 298 K does not change from 300 ps onwards and it converge to 25 at the end of simulation. Which indicates the stability of the system, and the reaction between the polymer chains does not occur. This is in agreement with the experimental observation in our previous experimental work 8, wherein we observed that, when the temperature is low, almost no reaction or only electrostatic interaction exists between the

C-PES and PEI, which resulted in very low salt rejection. On increasing the temperature, the total number of molecules decreased, which indicates that reactions occurred between the molecules during the MD simulation, and this trend is similar for the two temperatures of 323 and 353 K. Furthermore, the results show that, at the beginning of the MD simulation, the total number of molecules at 353 K is less than that at 323 K, but from 250 ps onwards, the total number of molecules increases as compared to that at 323 K, which could be because some reactions are reversible at 353 K. Finally, the simulation results indicate that the total number of molecules converge to 24 and 23 molecules, respectively, at 323, and 353 K.

The simulation results presented in Fig. 5b indicate that at first, the number of water molecules decreases during the MD simulation at 298 K, while after 500 ps, the number of water molecules in the simulation box becomes constant at 23 molecules. Moreover, the water molecules react with the PEI polymer chains, and the polymer chains are thus prepared to interact with each other. According to the simulation results, finally, the number of water molecules converge to 22, 19 and 20 molecules at 298, 323, and 353 K, respectively.

As shown in Fig. 5c, the type of molecules changes during the simulation, and finally, the number of types of molecules becomes constant at 3, 4, and 4 types of molecules at 298, 323, and 353 K, respectively. Further research on the type of molecules in the simulation shows that the maximum number of types of molecules in the simulation box is five at the beginning of the MD simulation, which is related to the decomposition or reaction of water molecules and the new O_2H_3

molecules or to the H+ and OH− that were produced. However, these new molecules are not stable during the MD simulation, and they finally react with each other to produce water molecules.

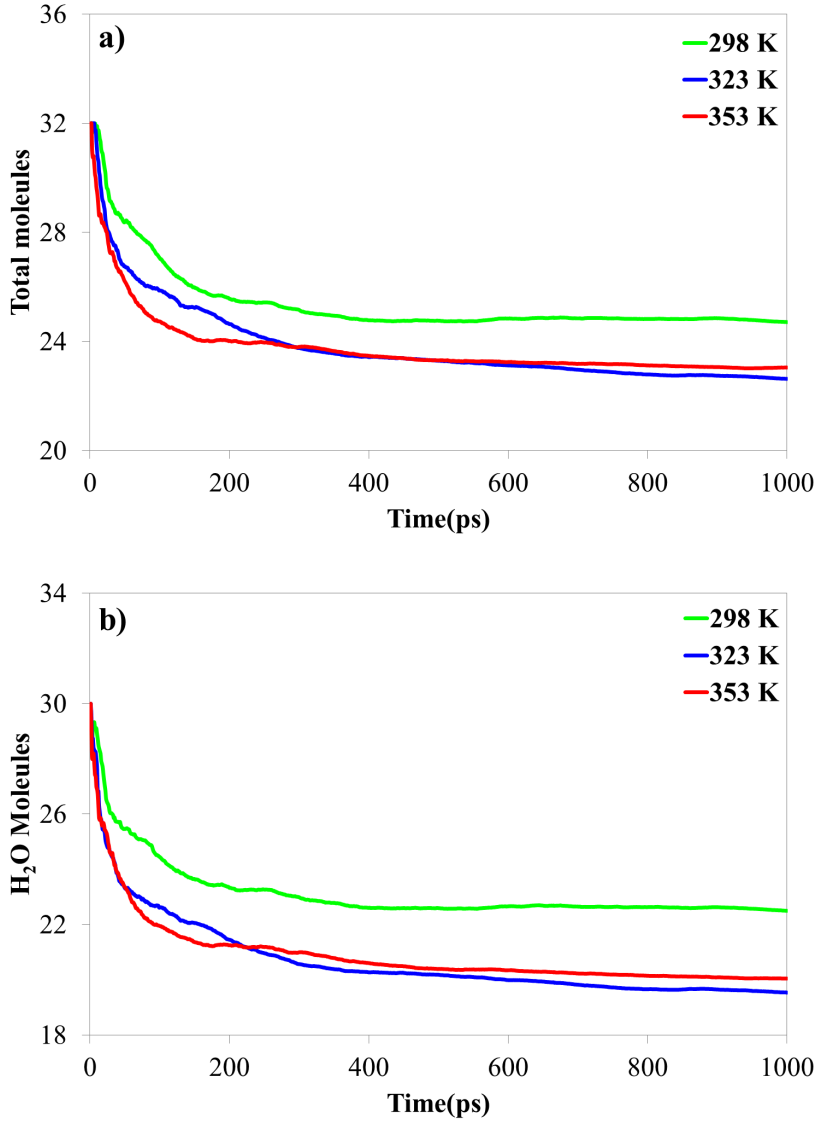

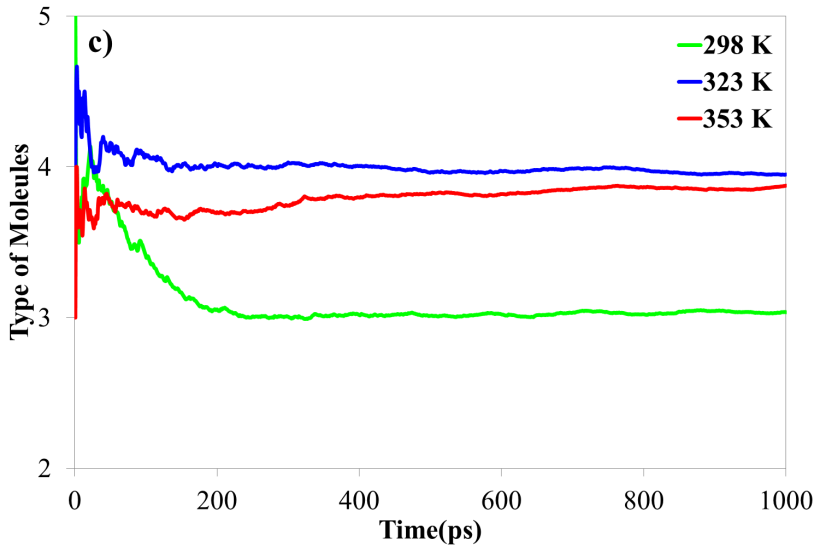

Fig. 5: Molecules versus time at various temperatures for a) total molecules in the simulation box; b) water molecules; and c) types of molecules.

The number of new molecules that resulted from the reaction of the PEI and C-PES molecules is calculated during the simulations at different temperatures, as shown in Fig. 6. At 298 K, the new molecule was formed from the reaction of the PEI and C-PES molecules after 100 ps, and the number of molecules is constant until the end of the simulation time. However, as the temperature increases to 323 K, the number of new molecule decreases and with a further increase in temperature to 353 K, the new molecules are unstable, and decomposition of the bonded chemicals occurs. Therefore, it can be said that, by increasing the temperature to 323 and 353 K, the probability of the PEI and C-PES molecules forming a chemical bond is low, and the produced molecules become unstable at a higher temperature. We hypothesised that the reacted molecules of C-PES and PEI decompose at high temperatures, and thus, the reaction becomes reversible. Thus, this results in defects in the selective dense layer of the NF membrane. This phenomenon was observed experimentally by Zarei et al. 8, which noticed that when temperature increased to

higher than a certain value, 343 K, the prepared membraned rejection decreased. They also hypothesised that reacted molecules of C-PES and PEI decompose at high temperatures.

In addition, the study of the bonds formed during the simulation at different temperatures demonstrates that, at 323 and 353 K, the CNH_2 group of PEI reacts with a COOH group of C-PES and forms a new bond and a molecule; however, at 298 K, this type of reaction is not observed, and a new molecule is observed in Fig. 6a owing to the proximity of the polymer chains and the interaction between the two groups of C_3N of PEI and the COOH of C-PES. Again these results are entirely in line with Zarei et al. 8 that they found by increasing temperature to a certain value membrane, the prepared nanofiltration membrane rejection increased. They attributed the increase in membrane rejection to the reaction between the CNH_2 group of PEI reacts with a COOH group of C-PES and the formation of a new bond and a molecule.

In a similar study, Akbarian et al. [42] utilised ReaxFF based molecular dynamics (MD) simulations and experimental techniques to obtain the effect of temperature on the peroxide-

induced crosslinking of polyethylene. MD results confirmed that high temperature had an adverse effect on the cross-linking, which is in accordance with the results of this work.

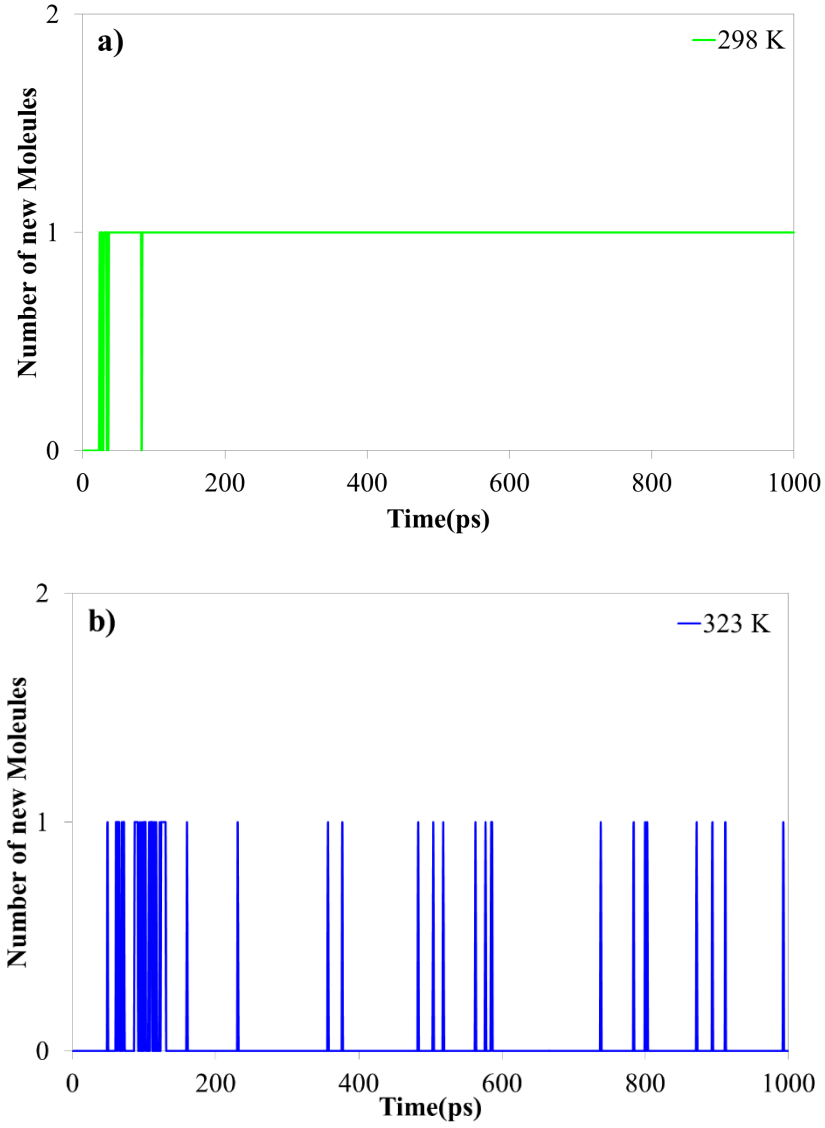

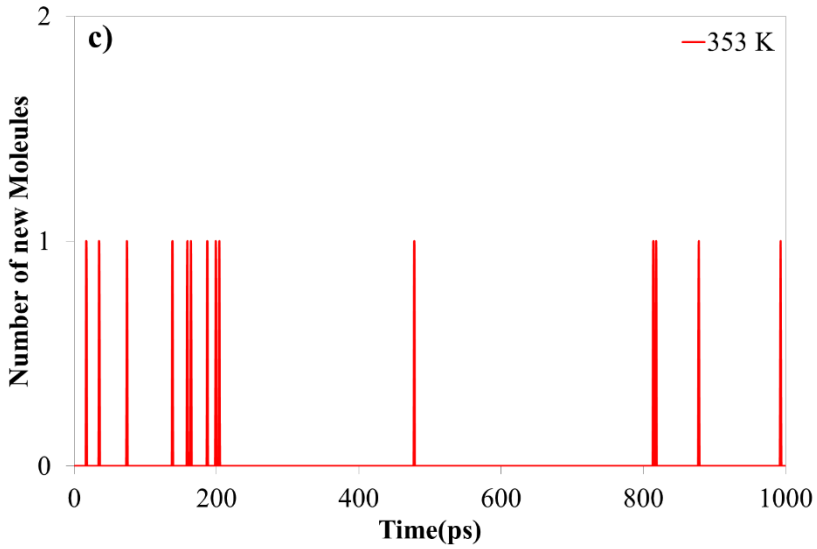

Fig. 6: Number of new molecules resulting from the reaction of the PEI and C-PES molecules at various temperatures: a) 298 K, b) 323 K, and c) 353 K.

The bonded and torsion energy of the molecules is calculated in the MD simulation at the beginning of the simulation (1 ns from the total simulation time) and can be observed in Fig. 7. The simulation results indicate that the value of the bond energy, which indicates the formation of new bonds between the molecules, and when this value is low, it indicates that more or stronger bonds have been formed between them. Furthermore, the simulation results in Fig. 7a indicate that the maximum and minimum bonded energies are observed at 298 and 323 K, respectively. Therefore, at 323 K, more or stronger bonds form between the molecules relative to the case of other temperatures. According to the simulation results in Fig. 7b, the torsion energy of the molecules increases during the simulation time, which is attributed to the change in the angle and the torsion of the molecules over time, to achieve a stable and an optimal position in the simulation box. Therefore, at 298 K, as compared to other temperatures, the torsion and rotation tendencies of the molecules are low. However, at 323 and 353 K, the interaction of the PEI and C-PES chains

is greater as they find suitable positions. Furthermore, at 353 K, the reversible reactions between the polymer chains increase the torsion energy.

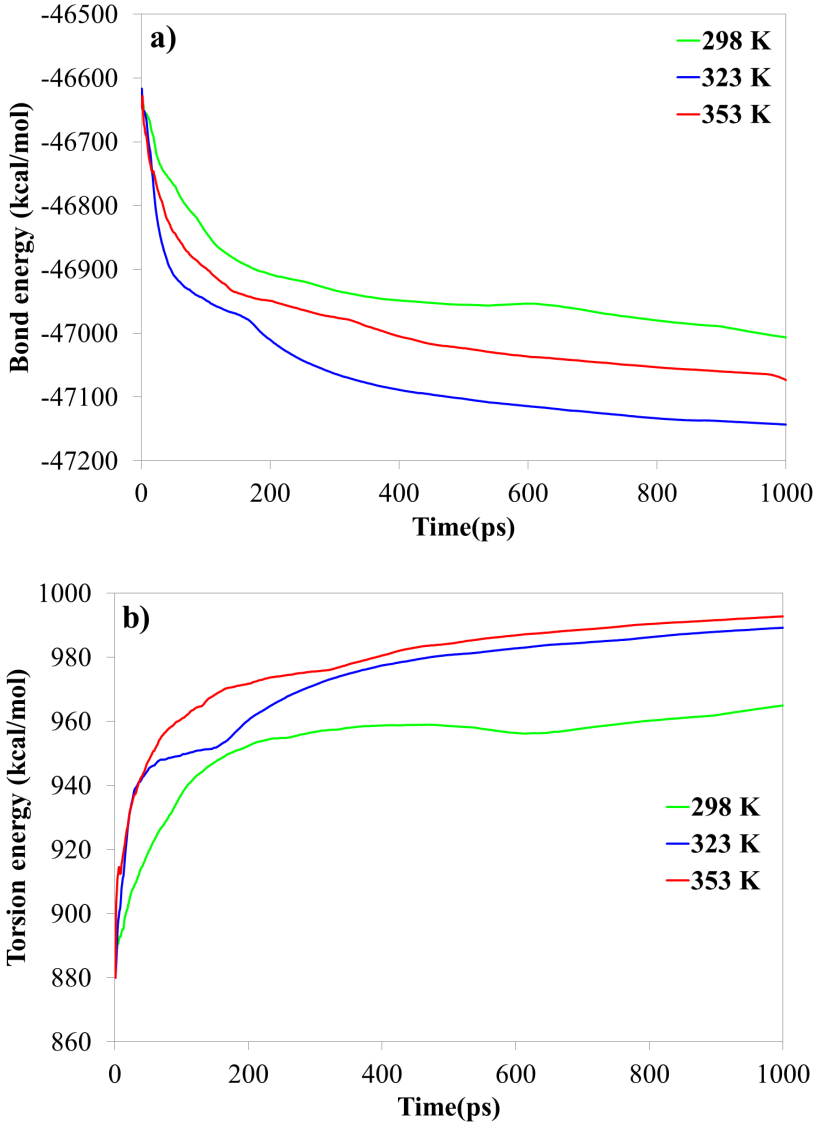

Fig. 7: Energy (kcal/mol) observed during the MD simulation at various temperatures: a) bonded energy; and b) torsion energy.

In these systems, the hydrogen bond plays an important role due to the presence of water molecules and oxygen and nitrogen atoms in the polymer chains. The hydrogen bond is formed

owing to the electrostatic interaction that occurs when a hydrogen atom (H) covalently bonds to other atoms of N or O. The hydrogen bond is stronger than the van der Waals interaction but weaker than the covalent or ionic bonds. Fig. 8 presents the variation of the hydrogen bond energy as a function of the simulation time at the beginning of the simulation (1 ns from the total simulation time). The simulation results indicate that the hydrogen bond energy decreases until it levels off after 100 ps at 298 and 323 K. The lowest hydrogen bond energy corresponds to the temperature of 298 K, which indicates the formation of the greatest number of hydrogen bonds at this temperature, and at 323 K, owing to the interaction between PEI and C-PES, the number of hydrogen bonds decreases, and the energy increases as compared to that at 298 K. Nevertheless, at 353 K, the hydrogen bond energy changes and increases at 100 ps as compared to that at other temperatures owing to the reversible reactions of the polymer chains as well as the effect of temperature on the hydrogen bond formation. In general, the simulation results in Fig. 8 indicate that the hydrogen bonds energy of the system decrease with increasing temperature because the enthalpy of hydrogen bond formation is usually negative. As was expected, the number of hydrogen bonds in blends of polymers[43,44] drop with the increasing temperature. Also, Hu et al.45 are reported that as the temperature increased, the hydrogen bonds decreased.

.

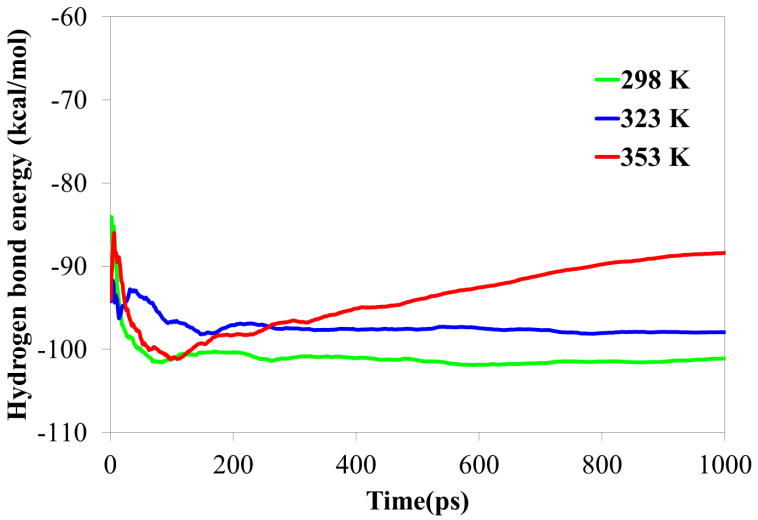

Fig. 8: Hydrogen bond energy as a function of the simulation time at various temperatures.

4. Conclusion

In this study, the interaction between the PEI and C-PES polymers in the presence of water molecules was investigated using an MD simulation. Initially, the comparison of the simulation results and experimental data showed that they have a good agreement. The effect of temperature on the interaction of two PEI and C-PES polymers at 298, 323, and 353 K was then investigated, and the results showed that, at 323 K, the reaction between the polymers occurs through the COOH group of C-PES and CNH_2 group of PEI, and as the temperature increases to 353 K, reversible reactions occur. These results are in good agreement with the experimental results obtained by us in a previously published papers [7-8]. The simulation results also showed that the interaction between the water molecules and N atoms in the PEI chain for the hydrogen bonding is high and decreases as the temperature increases. Finally, the simulation result indicates that the reversible reaction of the PEI and C-PES polymers that occurred at 353 K was also presented in a previously published papers.

References:

1. Ooi, B. S.; Sum, J. Y.; Beh, J. J.; Lau, W. J.; Lai, S. O. In Membrane Separation Principles and Applications; Ismail, A. F.; Rahman, M. A.; Othman, M. H. D.; Matsuura, T., Eds.; Elsevier, 2019.

2. Ghosh, A. K.; Hoek, E. M. V., Journal of Membrane Science 336, 140 2009.

3. Karan, S.; Jiang, Z. W.; Livingston, A. G., Science 348, 1347 2015.

4. Liu, C.; Shi, L.; Wang, R., Journal of Membrane Science 486, 169 2015.

5. Setiawan, L.; Shi, L.; Wang, R., Polymer 55, 1367 2014.

6. Lim, S. K.; Setiawan, L.; Bae, T. H.; Wang, R., Journal of Membrane Science 501, 152 2016.

7. Bagheri, M.; Rajabzadeh, S.; Elmarghany, M. R.; Moattari, R. M.; Bakhtiari, O.; Inada, A.; Matsuyama, H.; Mohammadi, T., Prog Org Coatings 1412020.

8. Zarei, F.; Moattari, R. M.; Rajabzadeh, S.; Bagheri, M.; Taghizadeh, A.; Mohammadi, T.; Matsuyama, H., Journal of Membrane Science 5882019.

9. Setiawan, L., Shi, L., & Wang, R., Polymer 55, 1367 2014.

10. Han, G., Chung, T. S., Weber, M., & Maletzko, C. , Environmental science & technology 52, 3676 2018.

11. Fang, W. X.; Shi, L.; Wang, R., Journal of Membrane Science 430, 129 2013.

12. Chen, T.; Yuen, A.; Lin, B.; Liu, L.; Lo, A.; Chan, Q.; Zhang, J.; Cheung, S.; Yeoh, G., Journal of Analytical and Applied Pyrolysis 153, 104931 2020.

13. Vashisth, A.; Ashraf, C.; Bakis, C. E.; Van Duin, A. American Society for Composites (ASC) 33rd Annual Technical Conference, the 18th US-Japan Conference on Composite Materials, and the ASTM D30, 2018.

14. Vashisth, A.; Ashraf, C.; Zhang, W.; Bakis, C. E.; Van Duin, A. C., The Journal of Physical Chemistry A 122, 6633 2018.

15. Aluko, O.; Gotham, S.; Odegard, G., Journal of Mechanics Engineering and Automation 5, 655 2015.

16. Odegard, G. M.; Jensen, B. D.; Gowtham, S.; Wu, J.; He, J.; Zhang, Z., Chemical Physics Letters 591, 175 2014.

17. Damirchi, B.; Radue, M.; Kanhaiya, K.; Heinz, H.; Odegard, G. M.; Van Duin, A. C., The Journal of Physical Chemistry C 124, 20488 2020.
18. Van Duin, A. C.; Merinov, B. V.; Han, S. S.; Dorso, C. O.; Goddard Iii, W. A., The Journal of Physical Chemistry A 112, 11414 2008.
19. Vashisth, A.; Ashraf, C.; Bakis, C. E.; van Duin, A. C., Polymer 158, 354 2018.
20. Hu, S.; Sun, W.; Fu, J.; Zhang, L.; Fan, Q.; Zhang, Z.; Wu, W.; Tang, Y., Journal of molecular modeling 23, 179 2017.
21. Hu, S.; Sun, W.; Fu, J.; Zhang, Z.; Wu, W.; Tang, Y., RSC advances 8, 3423 2018.
22. Pisani, W. A.; Radue, M. S.; Chinkanjanarot, S.; Bednarcyk, B. A.; Pineda, E. J.; Waters, K.; Pandey, R.; King, J. A.; Odegard, G. M., Polymer 163, 96 2019.
23. Chenoweth, K.; Cheung, S.; Van Duin, A. C.; Goddard, W. A.; Kober, E. M., Journal Of The American Chemical Society 127, 7192 2005.
24. Zhao, T.; Li, T.; Xin, Z.; Zou, L.; Zhang, L., Energy & fuels 32, 2156 2018.
25. Kim, S.-Y.; Van Duin, A. C., The Journal of Physical Chemistry A 117, 5655 2013.
26. Vashisth, A.; Kowalik, M.; Gerringer, J. C.; Ashraf, C.; Van Duin, A. C.; Green, M. J., ACS Applied Nano Materials 3, 1881 2020.
27. Soleymanibrojeni, M.; Shi, H.; Liu, F.; Han, E.-H., Computational Materials Science 173, 109424 2020.
28. Yilmaz, D. E.; van Duin, A. C., Polymer 154, 172 2018.
29. Shu, Y.; Wang, D.; Feng, B.; Liu, N.; Lu, Y.; Huo, J.; Yi, Y.; Bi, P.; Ding, X.; Shu, Y., Computational Materials Science 152, 158 2018.
30. Accelrys, Biovia Materials Studio, http://accelrys.com/products/collaborative-science/biovia-materials-studio
31. Navarro, R. R.; Sumi, K.; Fujii, N.; Matsumura, M., Water Research 30, 2488 1996.
32. Zhao, C.; Wei, Q.; Yang, K.; Liu, X.; Nomizu, M.; Nishi, N., Separation and purification technology 40, 297 2004.
33. Bahlakeh, G.; Nikazar, M.; Hafezi, M.-J.; Dashtimoghadam, E.; Hasani-Sadrabadi, M. M., International Journal of Hydrogen Energy 37, 10256 2012.
34. Khodaparast-Kazeroonian, F.; Amjad-Iranagh, S.; Modarress, H., International Journal of Hydrogen Energy 40, 15690 2015.

35. Hofmann, D. W.; Kuleshova, L.; D'Aguanno, B., Chemical Physics Letters 448, 138 2007.
36. Fogarty, J. C.; Aktulga, H. M.; Grama, A. Y.; Van Duin, A. C.; Pandit, S. A., The Journal of chemical physics 132, 174704 2010.
37. Huo, J.; Qi, W.; Zhu, H.; Yang, B.; He, G.; Bao, J.; Zhang, X.; Yan, X.; Gao, L.; Zhang, N., International Journal of Hydrogen Energy 44, 3760 2019.
38. Sprik, M.; Hutter, J.; Parrinello, M., The Journal of chemical physics 105, 1142 1996.
39. Soper, A., Chemical Physics 258, 121 2000.
40. Soper, A., The Journal of chemical physics 101, 6888 1994.
41. Blake, A. J.; Ebsworth, E.; Welch, A., Acta Crystallographica Section C: Crystal Structure Communications 40, 413 1984.
42. Akbarian, D.; Hamedi, H.; Damirchi, B.; Yilmaz, D. E.; Penrod, K.; Woodward, W. H.; Moore, J.; Lanagan, M. T.; van Duin, A. C., Polymer 183, 121901 2019.
43. Pehlert, G. J.; Painter, P. C.; Veytsman, B.; Coleman, M. M., Macromolecules 30, 3671 1997.
44. Hong, J.; Goh, S.; Lee, S.; Siow, K., Polymer 36, 143 1995.
45. Hu, Y.; Gamble, V.; Painter, P. C.; Coleman, M. M., Macromolecules 35, 1289 2002.